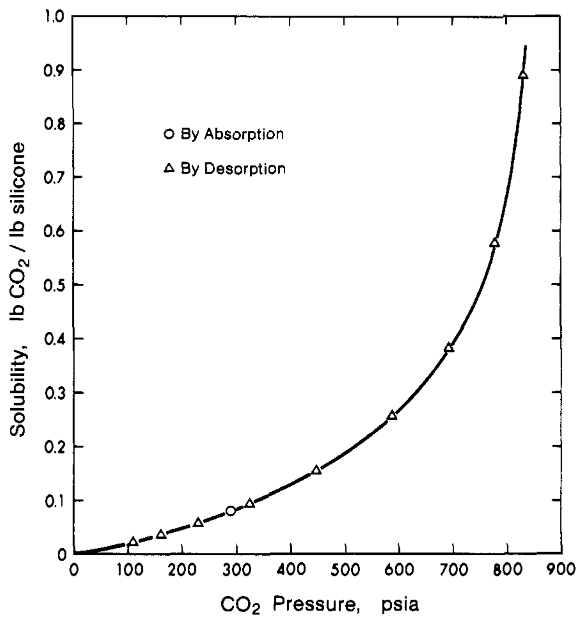

Figure 1.

In the temperature range below the first discontinuity the author states that the decomposition is represented solely by the reaction

$$2NaHCO_3(s) \rightarrow Na_2CO_3(s) + H_2O(g) + CO_2(g) \qquad (1)$$

and as such the phase rule dictates that the system contains only one degree of freedom.

However, an inspection of Figure 2 indicates that the dissociation pressure in this region is a function of both temperature and the ratio V_g/V_s. The author does not explain this discrepancy.

As shown in Figure 1 of Templeton's apparatus, a slug of silicone oil is used in the tube connecting the Heise gage to the heated bomb. In view of our results, if this quantity of silicone were large, appreciable quantities of CO_2 could be dissolved in the oil and the assumption of equimolar CO_2 and H_2O concentrations would be invalidated. Under these circumstances the system would contain a second degree of freedom and thus provide an explanation for the observed behavior.

The Peng-Robinson equation[7] predicts a dew point curve for an equimolar mixture of CO_2 and H_2O which may be represented by

$$\ln P = 16.9913 - 5074.96/T \qquad (2)$$

where P is pressure, psia, and T is temperature, K. Since most of Templeton's data are found to be at higher pressures than those predicted by eq 2, it appears that partial condensation also occurs inside the bomb.

While this latter consideration may prove to be the most significant source of discrepancy in this case, the general conclusions of this paper remain valid and careful consideration should be given to CO_2 solubility when relevant.

Literature Cited

(1) Templeton, C. C., *J. Chem. Eng. Data*, **23**, 7 (1978).
(2) Schiefer, H. M., Van Dyke, J., *ASLE Trans.*, **7**, 32 (1964).
(3) Schiefer, H. M., Azzam, H. T., Miller, J. W., *Lubr. Eng.*, **25**, 210 (1969).
(4) Dow Corning Corp. trade publication, "Information about Silicone Fluids", Form No. 22-053-76.
(5) Jacobsen, R. T., Stewart, R. B., *J. Phys. Chem. Ref. Data*, **2**, 757 (1973).
(6) Bishnoi, P. R., Miranda, R. D., Robinson, D. B., *Hydrocarbon Process.*, **53**, 197 (1974).
(7) Peng, D-Y., Robinson, D. B., *Ind. Eng. Chem. Fundam.*, **15**, 59 (1976).

Received for review January 8, 1979. Accepted May 3, 1979.

Solid Hydrocarbon Solubility in Liquid Methane–Ethane Mixtures along Three-Phase Solid–Liquid–Vapor Loci

David L. Tiffin, James P. Kohn,* and Kraemer D. Luks

Department of Chemical Engineering, University of Notre Dame, Notre Dame, Indiana 46556

Three ternary systems, methane–ethane–*n*-octane, methane–ethane–benzene, and methane–ethane–cyclohexane, are investigated along their three-phase S–L–V loci. The dramatic solubility enhancement of these solid hydrocarbons in liquid methane due to the presence of ethane is documented and presented graphically for a wide range of ethane concentration levels. Pressure, temperature, liquid-phase molar volume, and liquid-phase composition are tabulated in raw data form.

Introduction

Solid solubility data of hydrocarbon components in low molecular weight solvents are important for use in the design of liquefaction, vaporization, and transport systems for liquefied natural gas (LNG) and liquefied petroleum gas (LPG). The authors are engaged in an extended program of obtaining such data along solid–liquid–vapor loci, primarily in the low solute concentration range.

The solubility of hydrocarbons (*n*-pentane and higher) in liquid methane is quite low in methane-rich binary systems (for example, see ref 6 and 7); on the other hand, the solubility of these same hydrocarbons in liquid ethane (*5*, *10*) is considerably closer to ideal. It follows that, in a ternary S–L–V system with a solvent liquid mixture of methane and ethane, one would expect an increase in the solubility of the hydrocarbon solute over that of a binary system in which pure methane is the solvent liquid. However, it has been observed that, for modest additions of ethane, propane, or *n*-butane to liquid methane, the solubility of hydrocarbons is enhanced significantly beyond what one would reasonably expect by using simple combinatorial rules (*11*, *12*). The solubilities of the hydrocarbon solutes *n*-heptane and *n*-octane were studied in the solvent mixtures of methane–ethane in ref 12 and in solvent mixtures of methane–propane and of methane–*n*-butane in ref 11. In these studies, the data are tabulated, and the solute composition in the liquid phase is

0021-9568/79/1724-0306$01.00/0 © 1979 American Chemical Society

represented graphically as a function of temperature along constant solvent–solvent ratio S–L–V loci.

Other ternary S–L–V studies have concentrated exclusively on the solute CO_2. Kurata (*6*) investigated the solubility of solid CO_2 in solvent mixtures of methane–ethane, methane–propane, methane–*n*-butane, and ethane–propane. Clark and Din (*1*) studied the ternary S–L–V system ethane–ethylene–CO_2. Noteworthy is the observation that enhancement for the solute CO_2 is *not* significant for temperatures below 200 K (*6*).

Materials

The methane used in this study was Linde "Ultra Pure" grade stated to be 99.97 mol % pure. The ethane was a Matheson CP grade gas stated to be 99 mol % pure. The methane was used without further purification; however, the ethane was prepared for use by flashing it from the cylinder at room temperature to a 3000-cm^3 storage reservoir maintained at 0 °C. The vapor phase was then vented from the reservoir to remove the impurities remaining in the vapor phase after liquefaction from the cylinder. The ethane was further purified through active carbon before use.

Dew-point bubble-point experiments were carried out for both pure gases. For example, at -85.1 °C, methane exhibited a difference between dew-point and bubble-point pressures of less than 0.20 atm. The ethane had dew-point and bubble-point pressures which differed by 0.24 atm at 0.0 °C. The vapor pressure at 50 vol % liquid agreed well with recent literature values for both gases, and the critical temperature and pressure of the ethane were within 0.2 K and 0.1 atm of those given by the National Bureau of Standards (*2*).

The solvent mixtures were prepared from the pure solvent gases discussed above. To make the mixtures, we vented the pure gases into a bomb of known volume at a predetermined pressure and temperature. By venting the heavier gas in first, it was relatively easy to obtain approximately the desired solvent mixture. The bomb was then thermally mixed for 48 h before the contents were analyzed to obtain the composition of the solvents. The composition was determined by a Dumas bulb technique and checked by a gas chromatograph. There were a total of three methane–ethane mixtures used in this study and their compositions were 0.893, 0.790, and 0.892 mole fraction methane. The compositions are accurate to at least ±0.007 mole fraction methane.

The *n*-octane was manufactured by Humphrey-Wilkinson Chemical Co., the benzene was manufactured by Mallinckrodt Chemical Co., and the cyclohexane was an Eastman reagent. All had a stated purity of 99%. The measured air-saturated freezing points agreed to within 0.1 K of current literature vlaues for all three solute components, and measured refractive indices were within ±0.0003 of current literature values at 20 °C. The refractive indices were measured on a Bausch and Lomb Abbe-3L refractometer, which was accurate to ±0.0001. The purity of these hydrocarbons was further checked by use of a GOW-MAC Series 500 thermal conductivity gas chromatograph. Only trace impurities were found by injecting the samples through the GC column at 160 °C. The column was packed with 20 000 molecular weight Carbowax on Chromabsorb P. The hydrocarbon solutes were thus used without further purification.

Experimental Section

The apparatus and procedures used in this study are identical with that reported by Lee and Kohn (*7*) which was used in other cryoscopic studies (*3*, *4*, *8*). Briefly, the procedure involved charging a carefully weighed amount of liquid solute at room temperature to a glass equilibrium cell which had an inside volume from 10 to 24 mL and was calibrated for volumetric readings, either by visual observation or by use of a cathetometer. The air was vented from the cell by repeated flushing with the solvent mixture gas (a mixture of known methane/ethane ratio). The cell was thermostated in a liquid bath confined in a Dewar flask; the bath could be chilled by means of a cascade refrigerator or liquid N_2 or both. The solvent mixture gas was added to the cell from a reservoir using a calibrated positive displacement mercury pump. The bath was cooled slowly while agitation of the cell contents was effected by a steel ball actuated by an override magnet. The temperature was lowered until crystals formed and then was raised until only a trace of crystals remained. It was possible visually to detect as little as a few tenths of a milligram of crystals in the cell. This was regarded as an equilibrium crystal point with known liquid-phase solute composition. The distribution of methane and ethane between the liquid phase and the vapor space in the cell was determined with the aid of existing literature on methane–ethane vapor–liquid equilibria (*10*, *13*). (At a given temperature the ratio of methane-to-ethane in the liquid phase is dependent on the relative proportion of vapor-to-liquid phases in the cell. Since methane is more volatile than ethane, the liquid phase gets richer in methane as the cell fills but is always less than the batch ratio.) Addition of more solute mixture gas would lead to dissolution of the remaining crystals. The temperature would then be lowered until crystals again appeared, and the above procedure was followed for establishing the new equilibrium crystal point. When the cell filled with liquid phase, the "run" could be terminated.

Several "runs" with different solute loadings and different original solvent gas mixtures of varying methane–ethane ratios were made to cover a wide range of temperature and liquid-phase compositions.

Temperatures were taken on a platinum resistance thermometer which was accurate to at least ±0.03 K of the 1968 IPTS scale. Pressures were taken on a calibrated Heise Bourdon tube gage which was accurate to at least ±0.07 atm. Liquid-phase volumes could generally be read to ±0.02 mL.

During a run, careful venting of some of the gas phase (removing predominately methane) enriched the liquid in ethane, providing compositional flexibility on a solute-free basis, as well as extending the number of data points attainable in a row (i.e., for a single known loading of a given hydrocarbon solute). When the cell was full, gas was slowly bled off into a bomb of known volume. This bomb was completely evacuated by a vacuum pump before each filling of vented gas. Knowledge of the pressure, temperature, volume, and composition of the gas in the bomb would then permit calculation of the amount of each solvent gas vented from the cell. The pressure of this bomb was monitored by an Ashcroft 5-in. Bourdon pressure gage with a range from 0 to 100 psia, and the temperature of the bomb was monitored by a 12-in. mercury thermometer which could be read to ±0.1 K. The composition of the gas in the bomb was determined by Dumas bulb techniques.

Results

Table I presents raw experimental data for the ternary system methane–ethane–*n*-octane, Table II for the ternary system methane–ethane–benzene, and Table III for the methane–ethane–cyclohexane ternary system. The pressures are precise to ±0.1 atm, the temperatures to ±0.1 K, and the liquid-phase molar volume to ±1.0 mL/g-mol. Error analysis in similar systems suggests the reliability of these points is ±2% for the liquid-phase solute composition.

From the compositional data in Tables I, II, and III, it is possible to estimate constant-temperature solid–liquid–vapor loci of solute composition over a range of methane–ethane ratios in the liquid phase. Figures 1, 2, and 3 depict estimates of isothermal S–L–V loci of ln x_i vs. $\bar{X}_{ethane}$ (where x_i is the solute mole fraction in the liquid phase and $\bar{X}_{ethane}$ is the solute-free

Table I. Solid-Liquid-Vapor Three-Phase Raw Data for the Methane-Ethane-*n*-Octane Ternary System

			liquid-phase compn (mole fractions)			liquid-phase molar vol,
run	temp, K	pressure, atm	methane	ethane	*n*-octane	mL/g-mol
1	192.42	39.15	0.8742	0.1179	0.007 87	58.13
	188.55	35.68	0.8856	0.1090	0.005 54	56.16
2	188.65	35.41	0.8782	0.1163	0.005 54	56.20
3	185.59	31.81	0.8709	0.1240	0.005 08	55.03
	180.92	28.13	0.8840	0.1127	0.003 26	53.26
	178.93	26.57	0.8878	0.1095	0.002 74	52.20
	177.02	25.07	0.8902	0.1074	0.002 38	52.29
4	177.25	24.93	0.8812	0.1161	0.002 69	51.46
	175.13	23.44	0.8860	0.1119	0.002 14	50.92
	172.90	21.87	0.8883	0.1098	0.001 87	50.18
	170.52	20.24	0.8907	0.1078	0.001 52	49.44
5	179.21	26.16	0.8746	0.1214	0.003 99	52.12
	176.17	24.19	0.8859	0.1116	0.002 50	51.76
	174.18	22.76	0.8887	0.1092	0.002 12	50.82
	172.57	21.53	0.8908	0.1074	0.001 81	50.48
6	173.14	22.90	0.8738	0.1240	0.002 16	51.32
	170.29	19.56	0.8838	0.1147	0.001 55	49.67
	167.27	18.00	0.8871	0.1116	0.001 29	48.88
	164.72	16.36	0.8904	0.1086	0.001 00	48.26
	162.37	14.93	0.8920	0.1072	0.000 838	47.49
7	186.28	25.75	0.6776	0.2985	0.023 9	52.59
	182.66	24.93	0.7435	0.2448	0.011 7	52.17
	180.57	23.91	0.7604	0.2308	0.008 78	51.56
	178.56	22.75	0.7712	0.2218	0.006 97	51.26
	176.69	21.66	0.7783	0.2160	0.005 69	50.63
	174.96	20.71	0.7826	0.2125	0.004 88	50.26
	174.18	20.17	0.7846	0.2109	0.004 51	50.13
	173.89	19.08	0.7559	0.2389	0.005 21	49.76
	173.09	17.72	0.7197	0.2742	0.006 14	49.54
	171.77	15.74	0.6683	0.3243	0.007 43	48.99
	170.35	13.36	0.5947	0.3960	0.009 32	48.50
	168.90	10.23	0.4803	0.5074	0.012 3	48.76
	167.08	5.81	0.3131	0.6701	0.016 9	48.96
	167.44	9.48	0.4703	0.5185	0.011 1	48.21
	167.41	11.05	0.5436	0.4479	0.008 58	48.08
	167.06	11.87	0.5899	0.4032	0.006 99	47.76
	166.83	12.55	0.6300	0.3644	0.005 64	47.67
	166.21	12.75	0.6555	0.3397	0.004 79	47.57
	165.66	12.89	0.6729	0.3229	0.004 21	47.59

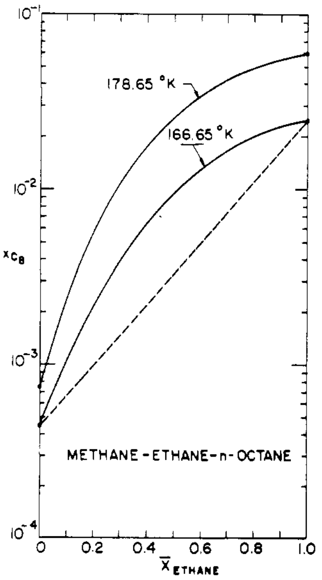

Figure 1. Estimates based on the data in Table I of the solid solubility of *n*-octane in the solid-liquid-vapor ternary system methane-ethane-*n*-octane with respect to $\bar{X}$, the solute-free ethane composition at T = 178.65 K and T = 166.65 K. The heavy dots (•) are the binary limits of the ternary data, and the dashed line represents a prediction that does not account for the ternary enhancement phenomena at 166.65 K.

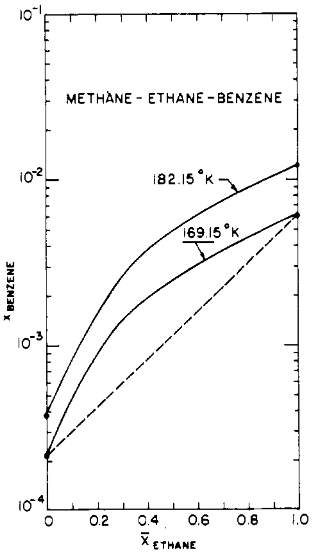

Figure 2. Estimates based on the data in Table II of the solid solubility of benzene in the solid-liquid-vapor ternary system methane-ethane-benzene with respect to $\bar{X}$, the solute-free ethane composition at T = 182.15 K and T = 169.15 K. The heavy dots (•) are the binary limits of the ternary data, and the dashed line represents a prediction that does not account for the ternary enhancement phenomena at 169.15 K.

mole fraction ethane in the liquid phase) based on the data for the three ternary systems studied. Figure 1 shows two solid-liquid-vapor isotherms for the ternary system methane-ethane-*n*-octane. The upper curve is at a temperature of 178.65 K and is based on three runs of data which varied in

Table II. Solid-Liquid-Vapor Three-Phase Raw Data for the Methane-Ethane-Benzene Ternary System

run	temp, K	pressure, atm	liquid-phase compn (mole fractions)			liquid-phase molar vol, mL/g-mol
			methane	ethane	benzene	
1	190.17	38.96	0.8820	0.1169	0.001 13	59.56
	184.65	31.68	0.8870	0.1122	0.000 845	50.22
	180.87	28.34	0.8898	0.1095	0.000 771	53.71
	181.90	27.53	0.8491	0.1498	0.001 13	52.58
	182.54	26.71	0.8158	0.1827	0.001 48	51.82
	182.35	24.40	0.7577	0.2403	0.002 05	50.58
	181.49	20.11	0.6426	0.3542	0.003 15	48.69
	179.94	22.36	0.7377	0.2604	0.001 93	49.98
	177.00	22.22	0.7974	0.2014	0.001 21	49.92
	174.17	21.13	0.8240	0.1751	0.000 899	49.74
	171.00	19.43	0.8408	0.1585	0.000 701	49.14
2	187.66	33.24	0.8618	0.1368	0.001 45	55.38
	182.67	29.36	0.8778	0.1213	0.000 965	53.99
	178.45	25.96	0.8832	0.1160	0.000 788	52.55
	172.82	21.81	0.8880	0.1114	0.000 613	50.82
	168.05	18.68	0.8910	0.1085	0.000 474	49.41
	168.36	18.27	0.8729	0.1265	0.000 575	49.06
	169.44	18.68	0.8596	0.1398	0.000 643	49.29
	170.55	18.48	0.8229	0.1724	0.000 841	49.09
	169.98	16.64	0.6600	0.3385	0.001 49	60.37
	169.80	13.44	0.4507	0.5465	0.002 92	71.14
	168.85	15.14	0.6524	0.3460	0.001 58	60.01
	165.47	14.87	0.7718	0.2273	0.000 807	53.99
	162.05	13.71	0.8105	0.1890	0.000 560	51.25
	160.38	13.10	0.8217	0.1778	0.000 488	50.38
3	187.18	25.01	0.6731	0.3230	0.003 90	50.16
	183.18	23.79	0.7146	0.2827	0.002 67	49.38
	174.70	19.57	0.7591	0.2394	0.001 48	48.52
	168.97	16.57	0.7746	0.2244	0.001 06	47.15
	165.00	14.40	0.7814	0.2177	0.000 826	46.83
	160.64	12.35	0.7861	0.2133	0.000 655	46.22
	156.73	10.59	0.7888	0.2106	0.000 531	45.74

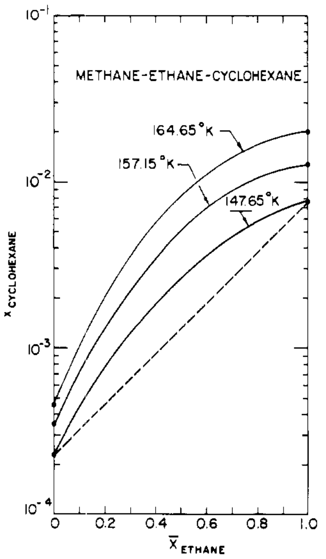

Figure 3. Estimates based on the data in Table III of the solid solubility of cyclohexane in the solid–liquid–vapor ternary system methane–ethane–cyclohexane with respect to $\bar{X}$, the solute-free ethane composition at $T = 164.65$ K, $T = 157.15$ K, and $T = 147.65$ K. The heavy dots (•) are the binary limits of the ternary data, and the dashed line represents a prediction that does not account for the ternary enhancement phenomena at 147.65 K.

solute-free composition from 0.11 to 0.23 mole fraction ethane. The lower curve in Figure 1 is at a temperature of 166.65 K and is based on a large number of data points ranging in solute-free mole fraction ethane from 0.11 to 0.70. Figure 2 has curves at temperatures of 182.15 and 169.15 K for the methane–ethane–benzene ternary system. These curves originated from three runs of ternary data which spanned the range of solute-free ethane mole fraction from 0.11 to 0.55. In the case of methane–ethane–cyclohexane (see Figure 3), there are three isotherms constructed from three runs of data which have solute-free ethane mole fractions in the liquid phase between 0.11 and 0.36. The curves in Figure 3 are at temperatures of 164.65, 157.15, and 147.65 K.

The binary end points of the curves in Figures 1–3 originated from several sources. The methane–*n*-octane and methane–cyclohexane systems are reported in ref 4. The methane–benzene binary points are extrapolations of Kuebler and McKinley's solid–liquid data (*5*) to the saturation pressure of pure methane. The ethane–*n*-octane end points are from ref 3 and the ethane–benzene and ethane–cyclohexane binary points from ref 8. On Figures 1–3, there is a dashed straight line drawn between the two binary S-L-V solubility limits at the lowest temperature isotherm for each of these three systems. These dashed lines are a representation of the solubility predicted from use of simple combinatorial rules in a Henry's law based equation to describe solid solubility. This equation is (*9*)

$$\ln x_i = \frac{\Delta h_i^\infty}{RT_t}\left[1 - \frac{T_t}{T}\right] - c_i \tag{1}$$

where Δh_i^∞ = enthalpy of solution of solute i in the solvent at infinite dilution and c_i = intercept in Henry's convention for solute i. If the constants Δh_i^∞ and c_i are arithmetically averaged over the solute-free solvent composition, as

$$\Delta h_i^\infty = \sum_j \bar{X}_j(\Delta h_i^{(j)\infty}) \tag{2}$$

and

$$c_i = \sum_j \bar{X}_j c_i^{(j)\infty} \tag{3}$$

one would arrive at

$$\ln x_i = \bar{X}_1 \ln x_i^{(1)} + \bar{X}_2 \ln x_i^{(2)} \tag{4}$$

where $\bar{X}_j$ = liquid-phase solute-free mole fraction of solvent j and $x_i^{(j)}$ = liquid-phase solute mole fraction in pure component

Table III. Solid-Liquid-Vapor Three-Phase Raw Data for the Methane-Ethane-Cyclohexane Ternary System

run	temp, K	pressure, atm	liquid-phase compn (mole fractions)			liquid-phase molar vol, mL/g-mol
			methane	ethane	cyclohexane	
1	177.85	22.89	0.7432	0.1949	0.061 9	51.42
	176.43	23.16	0.8212	0.1487	0.030 1	50.83
	171.46	20.24	0.8572	0.1259	0.016 9	48.30
	167.59	17.92	0.8659	0.1201	0.014 0	49.16
	163.16	15.40	0.8748	0.1145	0.010 7	47.04
	161.18	14.25	0.8780	0.1125	0.009 46	47.26
	157.79	12.55	0.8816	0.1104	0.008 00	46.65
	155.25	11.25	0.8840	0.1092	0.006 86	46.10
	156.97	10.91	0.8011	0.1860	0.012 9	46.34
2	176.46	20.51	0.6672	0.2479	0.084 9	51.10
	174.70	21.73	0.8153	0.1570	0.027 7	50.21
	171.36	19.96	0.8429	0.1380	0.019 1	49.53
	170.12	19.28	0.8570	0.1285	0.014 5	49.11
	164.98	16.22	0.8674	0.1210	0.011 7	48.11
	160.59	13.30	0.8777	0.1138	0.008 50	46.76
	156.03	11.53	0.8819	0.1111	0.007 04	46.03
	152.09	9.83	0.8858	0.1089	0.005 35	45.24
	147.22	7.92	0.8880	0.1079	0.004 08	44.32
	148.55	8.26	0.8720	0.1232	0.004 77	44.23
	147.98	7.78	0.8487	0.1455	0.005 81	44.05
	148.46	7.58	0.8140	0.1786	0.007 42	44.02
	147.99	6.90	0.7496	0.2402	0.010 2	43.70
	146.08	5.27	0.6325	0.3519	0.015 5	43.24
	143.78	5.74	0.7703	0.2224	0.007 33	43.05
	141.36	5.47	0.8101	0.1850	0.004 98	42.72
	139.30	5.06	0.8287	0.1675	0.003 88	42.45
3	170.08	13.68	0.5158	0.3808	0.103 5	53.15
	166.33	14.23	0.6959	0.2689	0.035 2	48.13
	163.06	13.07	0.7278	0.2471	0.025 1	48.58
	158.59	11.17	0.7570	0.2271	0.016 0	46.92
	153.62	9.26	0.7690	0.2187	0.012 2	46.05
	150.72	8.24	0.7765	0.2142	0.009 30	45.36
	146.88	6.95	0.7807	0.2117	0.007 64	44.79
	143.14	5.86	0.7839	0.2100	0.006 09	44.01
	143.07	5.52	0.7484	0.2445	0.007 17	44.00
	142.51	5.18	0.7021	0.2893	0.008 58	43.98
	141.74	4.50	0.6516	0.3303	0.010 1	43.90
	138.48	4.16	0.6962	0.2969	0.006 94	43.33
	136.30	3.75	0.7180	0.2766	0.005 38	43.08

j for a binary system at a constant temperature. Equation 4 is the dashed line at the lowest temperature in Figures 1–3. Deviation from such a line highlights the magnitude of the enhancement phenomena demonstrated by the actual data.

Glossary

c_i	triple point intercept in Henry's convention for solute i
$c_i^{(j)}$	binary triple point intercept in Henry's convention for solute i in solvent j
Δh_i^{∞}	enthalpy of solution of solute i at infinite dilution along S–L–V locus
$\Delta h_i^{(j)\infty}$	binary enthalpy of solution of solute i in solvent j at infinite dilution along S–L–V locus
L	liquid phase
R	universal gas law constant (1.987 cal/(g-mol K))
S	solid phase
T	temperature
T_t	triple point temperature (216.38 K for *n*-octane, 278.69 K for benzene, and 279.83 K for cyclohexane)
V	vapor phase
x_i	liquid-phase mole fraction of solute i
$x_i^{(j)}$	binary system liquid phase mole fraction of solute i in solvent j
$\bar{X}_j$	liquid-phase solute-free mole fraction of solvent j

Subscripts and Superscripts

i	denotes solute
j	denotes solvent
∞	infinite dilution

Literature Cited

(1) Clark, A. M., Din, F., *Trans. Faraday Soc.*, **49**, 202 (1953).
(2) Goodwin, R. D., Roder, H. M., Straty, G. C., "Thermophysical Properties of Ethane, from 90 to 600 K at Pressures to 700 Bar", *Natl. Bur. Stand.* (*U.S.*), *Tech. Note*, **No. 684** (1976).
(3) Kohn, J. P., Luks, K. D., Liu, P. H., *J. Chem. Eng. Data*, **21**, 360 (1976).
(4) Kohn, J. P., Luks, K. D., Liu, P. H., Tiffin, D. L., *J. Chem. Eng. Data*, **22**, 419 (1977).
(5) Kuebler, G. P., McKinley, C., *Adv. Cryog. Eng.*, **19**, 320 (1974).
(6) Kurata, F., "Solubility of Solid Carbon Dioxide in Pure Light Hydrocarbons and Mixtures of Light Hydrocarbons", GPA Research Report RR-10 (1974).
(7) Lee, K. H., Kohn, J. P., *J. Chem. Eng. Data*, **14**, 292 (1969).
(8) Liu, P. H., Luks, K. D., Kohn, J. P., *J. Chem. Eng. Data*, **22**, 220 (1977).
(9) Luks, K. D., Kohn, J. P., Liu, P. H., Kulkarni, A. A., *Hydrocarbon Process.*, **54**, 181 (1975).
(10) Michels, A., Nederbragt, G. W., *Physica* (*The Hague*), 656 (1939).
(11) Orozco, C. E., Tiffin, D. L., Luks, K. D., Kohn, J. P., *Hydrocarbon Process.*, **56**, 325 (1977).
(12) Tiffin, D. L., Luks, K. D., Kohn, J. P., *Adv. Cryog. Eng.*, **23**, 538 (1978).
(13) Wichterle, I., Kobayashi, R., *J. Chem. Eng. Data*, **17**, 9 (1972).

Received for review December 18, 1978. Accepted June 1, 1979. The authors are grateful for support of this work provided by the National Science Foundation (Grant No. ENG. 76-14391). The research equipment had been built under earlier grants from the National Science Foundation.